19th Brazilian Congress of Thermal Sciences and Engineering
November 06th-10th, 2022, Bento Gonçalves - RS - Brazil

ENC-2022-0669
RHEOLOGICAL STUDY OF HYDRATE SLURRIES IN WATER-BASED DRILLING FLUIDS

Guilherme Mühlstedt
Academic Department of Mechanics – DAMEC, Postgraduate Program in Mechanical and Materials Engineering – PPGEM, Research Center for Rheology and Non-Newtonian Fluids – CERNN, Federal University of Technology – Paraná – UTFPR, Brazil
muhlstedt@alunos.utfpr.edu.br

Diogo Elias da Vinha Andrade
Department of Mechanical Engineering – DEMEC, Rheology and Non-Newtonian Fluid Flow Laboratory –ReoSul, Federal University of Rio Grande do Sul – UFRGS, Brazil
diogo.andrade@ufrgs.br

Cezar Otaviano Ribeiro Negrão
Academic Department of Mechanics – DAMEC, Postgraduate Program in Mechanical and Materials Engineering – PPGEM, Research Center for Rheology and Non-Newtonian Fluids – CERNN, Federal University of Technology – Paraná – UTFPR, Brazil
negrao@utfpr.edu.br

Abstract. *One of the major risks in deep-water operations is the hydrate formation due to harsh conditions such as high pressure and low temperature. Hydrates are crystalline structures resembling ice that are formed by small molecules, such as light hydrocarbons, occluded in a cage-like structures composed of water molecules. Unexpected events such as a hydrocarbon influx to the wellbore during drilling procedures might result in hydrate formation in the water-based drilling fluid. Understanding the rheological properties of the system is crucial for ensuring suspension transportability or an eventual breakage of agglomerates jammed along the process. In this work, the rheological influence of the hydrate formation in a water-based drilling fluid, mainly composed of water (79%) and sodium chloride (14%), provided by Petrobras, was investigated under static and dynamic conditions. Tetrahydrofuran (THF) was used as a guest fluid. The guest fluid cut was set to hydrate structures not exceeding 40% in volume to ensure that the sample behaves as a liquid suspension. Rheometric tests revealed that the slurry formed by the suspension of hydrate crystalline structures was a time-dependent elasto-viscoplastic material in which the microstructure is irreversibly affected by the imposed shear.*

Keywords: *rheology, well drilling, drilling fluid, hydrates, hydrate slurry flow*

1. INTRODUCTION

Gas hydrates have been recognized as an issue by the oil and gas companies since the 1930s, when Hammerschmidt (1934) reported that hydrates were blocking gas transmission lines. Hydrates presence can decrease or block the oil and gas flow by forming a plug and they also represent a safety risk to the pipeline, platform and crew if there is a pressure build-up, since the plug can behave as projectiles (Sloan, 2010). Flow assurance was identified as the primary technical issue of offshore production by 110 energy companies at the turn of the century (Sloan, 2005).

With rising demand, oil and gas exploration is shifting to deep and ultradeep-water fields. High pressures and low temperatures found in such deep water are ideal for gas hydrate formation in both oil drilling (Østergaard et al., 2000) and production (Sloan and Koh, 2007). Millions of dollars have been spent to either thermally insulate flow lines (Liu et al., 2019) or inject additives (thermodynamics, kinetics, and antiagglomerant inhibitors) into the fluid to prevent and/or control hydrate formation (Østergaard et al., 2000; Kelland et al., 2008; Bavoh et al., 2020). Despite these precautions, unexpected conditions in the oil drilling process can favor hydrate formation.

In drilling hydraulics, gas hydrates can be formed when light hydrocarbon flows into the wellbore as a result of a gas kick (Østergaard et al., 2000; Botrel, 2001). Depending on the size, the hydrate crystals may form a suspension with the drilling fluid or may obstruct the annular space, the BOP stack, and the kill and choke lines or may even impair the drill string movement (Botrel, 2001; Liu et al., 2019). High pumping pressures that may damage the formation walls at

the well bottom may be required not only to remove plugs or hydrate slurries but also to break up the crystallized material and resume flow.

Due to the high costs of preventing hydrate formation and the lack of literature information, this study investigates the rheological properties of hydrate slurries in water-based drilling fluid. The shear influence on microstructure and system brittleness during hydrate formation, as well as the shear history influence on microstructure and system brittleness, were investigated.

2. EXPERIMENTAL SECTION

2.1 Materials

The tetrahydrofuran (THF) was used as guest fluid because of its unique properties: (i) being liquid at atmospheric conditions; (ii) completely soluble in water; (iii) and forming hydrates at atmospheric pressure. Unlike hydrophobic hydrate compounds, THF-water solution allows hydrate crystals to form and grow anywhere (Iida et al., 2001).

The THF (from Sigma-Aldrich, 99% purity) was added to a water-based drilling fluid (1160 kg/m^3 density) provided by Petrobras. The fluid is mainly composed of water (79%) and sodium chloride (14%). Other components of the drilling fluid are limestone, HP starch, lubricant, xanthan gum, magnesium oxide, magnesium peroxide, antibacterial, and antifoam.

2.2 Apparatus

The rheometric tests were performed using a Haake Mars III (Haake Co., Germany) stress- controlled rotational rheometer that can control the shear rate indirectly by a feedback PID controller and can measure a minimum and a maximum torque of, respectively, 1×10^{-8} and 2×10^{-1} Nm.

As apparent wall slip is a concern in rheological tests of hydrate slurries (de Lima Silva et al., 2017; Ahuja et al., 2015; Peixinho et al., 2010), two different sensors were employed in the experiments: a Couette geometry with a serrated surface cup (internal cylinder diameter of 25 mm, length of 40 mm, cup diameter of 26 mm, and 0.5 mm groove depth) and a four-blade Vane geometry (cup diameter of 27.2 mm, vane diameter of 22 mm, and length of 16 mm) with a piece of waterproof sandpaper glued on the cup wall to prevent wall slip, as proposed by Ahuja et al. (2015). The sandpaper reduces the effective cup diameter to 25.7 mm which was considered in the data analysis. The system temperature was controlled by a Peltier thermostatic bath system.

2.3 Methods

Before each experiment, the drilling sample was vigorously mixed to homogenize de fluid, then the experimental amount was separated. In a water−THF system, the hydrate forms the sII structure with a molar ratio of 1:17, meaning a mass fraction of about 19.08 wt% (Iida et al., 2001). To obtain roughly a 40% volume fraction of the solid hydrate in the system, 6.94 wt% THF at ambient temperature was added to the drilling fluid and gently mixed until total solubility in the drilling fluid and the sample was finally poured into the cup that was already at 5 °C. The rotor was lowered to its measuring position, the sample hood was attached to the system, and the rheometric test was then performed. In all the experiments, the sample was cooled from 5 to −10 °C with a cooling rate of 1.5 °C/min, and all the tests were performed at −10 °C.

Despite the experimental temperature was −10 °C, the amount of salt in sample prevents ice formation. To ensure that, the drilling fluid was tested without THF not only in rheometer, but also in a calorimeter and could not be observed any crystallization during the tests.

3. RESULTS AND DISCUSSION

3.1 Hydrate Formation During the Flow

The formation of hydrates in drilling fluid during flow was first investigated. Using the Couette geometry, the shear influence on hydrate formation was observed by imposing different shear rates. Figure 1 depicts the shear stress increasing during cooling for all applied shear rates, indicating an increase in the apparent viscosity of the material. After reaching -10 °C, the stress tends to stabilize before undergoing a significant change associated with hydrate formation. The higher the shear rate, the shorter the induction period (the time required for hydrate formation) and the time required for the stress to reach a steady state. While steady state is reached in 10 min for a shear rate of 100 s^{-1}, it takes 20 min for 30 s^{-1} and it is never achieved within 1 h of testing for 3 s^{-1}.

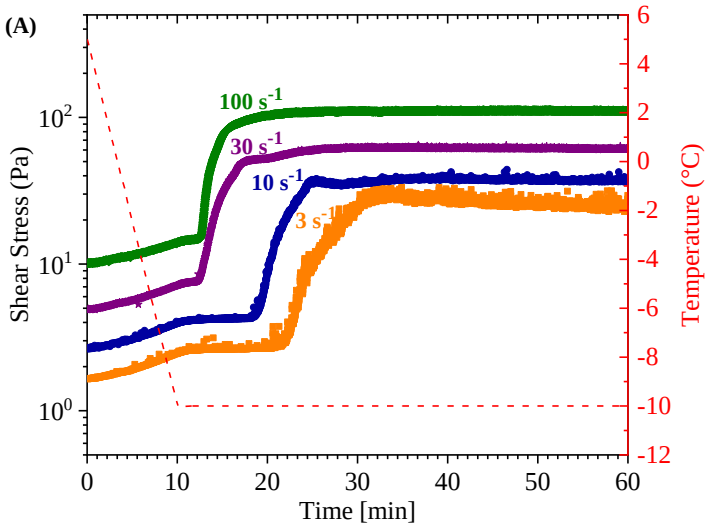

Figure 1. Shear stress as a function of time during hydrate formation for different imposed shear rates.

The effect of shear history on material rheology is now discussed. After cooling the sample to -10 °C with a constant shear rate of 3 s^{-1}, the sample was held at -10 °C for 60 min and sheared at 3 s^{-1}. The shear rate was then increased and maintained for another 60 min, and the step-up procedure was repeated every 60 mins until the limit of 100 s^{-1} was reached. The black line in Fig. 2 depicts the start of a shear step-down course to the limit of 3 s^{-1}. In the figure, the blue line represents the measured shear stress as a function of time.

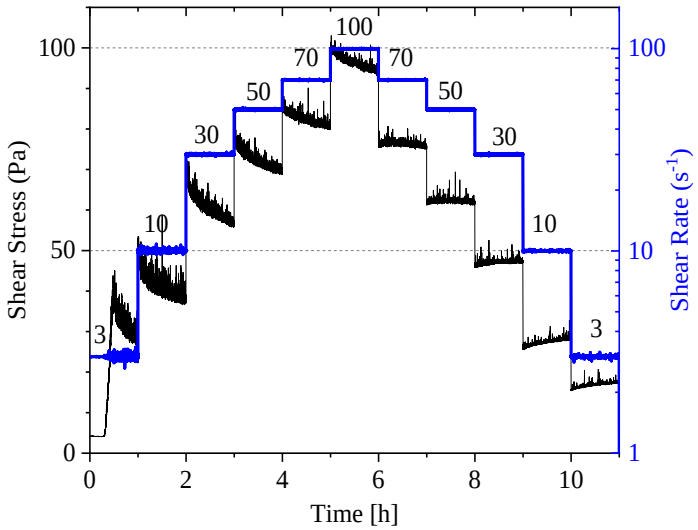

Figure 2. Shear stress (blue line) and shear rate (black line) as a function of time for hydrate slurries in drilling fluid.

As can be seen, there is a sudden increase in stress during the first shear rate plateau caused by hydrate formation. Due to the stochastic nature of hydrate nucleation and growth, the induction time and shear stress measured at 3 s^{-1} do not correspond to the values of the orange line in Fig. 1. Nevertheless, the transient response and shear stress measured after 1 hour of shear were nearly identical in both experiments. During the 3 s^{-1} shear rate period, the material shear stress decreases monotonically after hydrate formation.

After each shear rate step-up, a stress overshoot was observed followed by a continuous stress reduction (see Fig. 2), indicating that the 60-minute shearing period was insufficient for the stress to reach the steady state at any shear rate. A comparison of the stress obtained after increasing the shear rate to 10 s^{-1} with the stress obtained during hydrate formation at 10 s^{-1}, depicted in Fig. 1, shows that the first does not reach the steady state after 1 h of shearing, whereas the second does quite quickly, indicating that the magnitude of shearing applied during hydrate formation affects the material structure. The more structured the hydrate, the lower the shear rate during hydrate formation.

In contrast to the step-up period, stress undershoots, which are less noticeable than overshoots, are observed after shear rate abrupt reductions, with the stress gradually tending to equilibrium. The material structure cannot be

completely recovered during the step-down because the stress measured during the step-down period never reaches the same stress level obtained during the step-up period for the same shear rate. In other words, the maximum shear rate applied to the material breaks down the hydrate particles into smaller size aggregates, resulting in an irreversible reduction in apparent viscosity.

The stresses measured at the end of each shear rate-60 min plateau (Fig. 2) were plotted as a function of the shear rate in Fig. 3. Furthermore, the hollow diamonds in orange exhibit tensile strength at the end of each curve of hydration formation over a constant shear rate, as shown in Fig. 1. Finally, a drilling fluid flow curve without THF was plotted as a comparison.

The dashed lines in Fig. 3 are fitted curves for step-up and step-down curves (in blue) and the hydrate-free drilling fluid sample (in red). The Herschel-Bulkley equations in the figure demonstrate that the parameters fitted to both curves are strongly influenced by the sample's maximum shear rate. The dynamic yield stress, for example, declined from 20.5 to 9.9 Pa. In practice, hydrate slurries that have previously been sheared at high shear rates require lower pumping pressures than those that have only been mildly sheared. The flow curve for the drilling fluid at the same temperature (red squares) is presented alongside a fitted Power-Law fitting. This best-fitting power law implies that the fluid is a non-yield stress material.

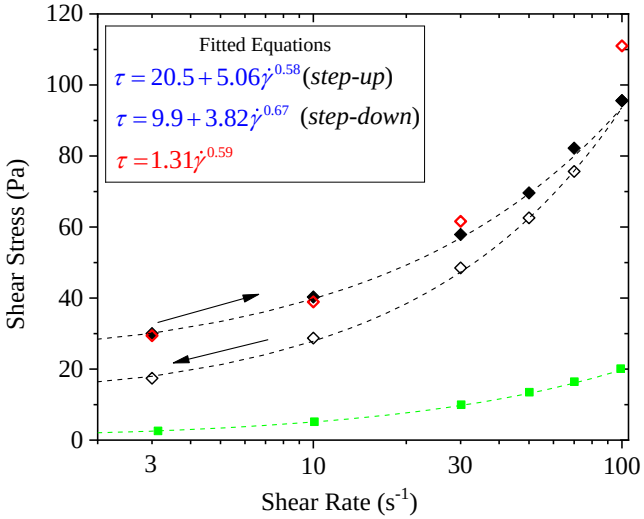

Figure 3. Flow curves for hydrate slurries: (i) in shear rate step-up and step-down (filled and the hollow blue diamonds, respectively); (ii) imposing constant shear rates obtained after 1 h of shearing in Fig. 1 (orange diamonds) and hydrate-free drilling fluid sample (red squares).

3.2 Hydrate Formation During Stoppage and the Flow Startup

In addition to the viscosity, the flow startup of the hydrate slurry after a shutdown is also investigated. Stress-controlled creep tests were firstly used to evaluate the flow startup. The hydrate was formed by imposing a shear rate of 100 s^{-1} for 1 h and then left aging for 10 min. After aging, the sample was submitted to a constant shear stress. Figure 4 shows the measured strain as a function of time for each creep test. While the stress was equal to or less than 10 Pa, the strain increased to a certain amount and then remained nearly constant, suggesting a solid-like material behavior. When the strain reached 13 Pa or above, it increased dramatically with time, indicating material breakage. As noted, the higher the stress, the faster the material breaks down. The material static yield stress for this 10 min aging experiment was between 10 and 13 Pa, which was higher than the dynamic yield stress determined from the material flow curve with the same maximum shear rate applied to the sample (as expected for time-dependent materials).

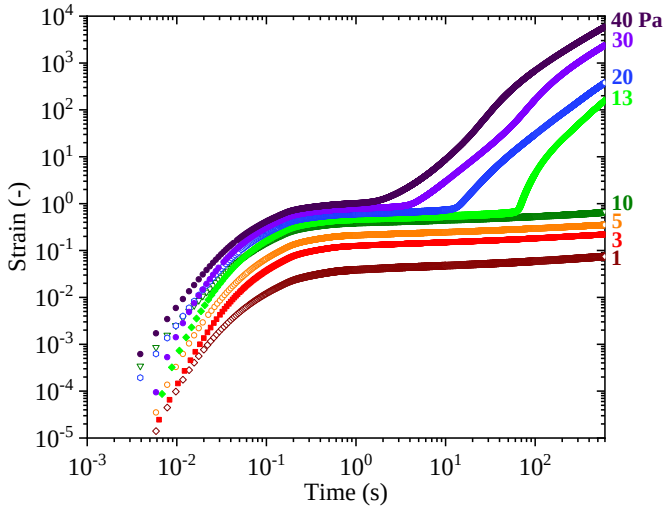

Figure 4. Shear strain as a function of time for creep tests at different stress levels (indicated next to each curve).

Another method for determining static yield stress is the ramp test which consists of a steady increase in stress and strain measurement. It is worth mentioning that in the solid-to-liquid phase, low deformation levels are measured, whereas rapid strain changes are observed as the material yields. This procedure was also used by Qin et al. (2017) to determine the yield stress of gas hydrate-in-oil slurries.

Figure 5 shows the stress ramp results for the drilling fluid (THF-free) solution in (red curve), hydrate slurries dynamically formed (blue curves) and statically formed (black curve). The samples that hydrates were formed as described for creep tests and were submitted to a three different aging times (10, 60 and 120 min). The hydrate slurry formed statically (black curve), was obtained with no shear imposed during the hydrate formation (for this test, a vane geometry was used).

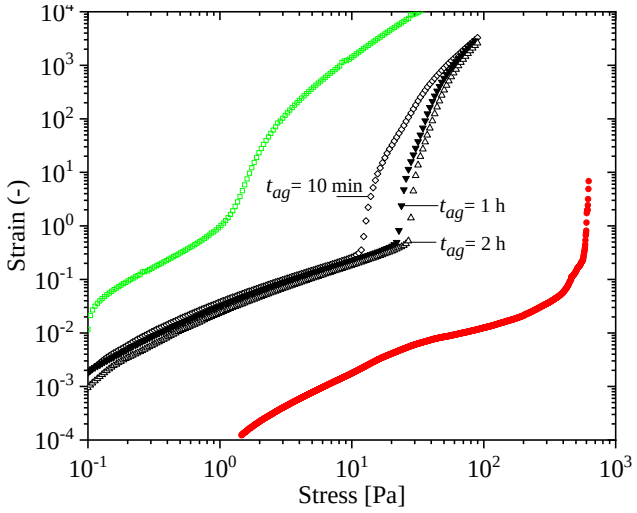

Figure 5. Strain as a function of stress for stress ramp test. (i) the hydrate-free sample after shearing at 100 s^{-1} for 10 min and 10 min of aging time (red circles); (ii) the hydrate slurry after shearing at 100 s^{-1} for 10 min and aging time of 10 min (blue diamonds), 1 h (blue down- triangles), and 2 h (blue up- triangles), respectively; and (iii) the hydrate slurry formed statically (black squares).

As noted in Fig. (5), the stress that abruptly increased the strain for an aging time of 10 min was approximately 10 Pa, which was roughly the same value obtained from creep test shown in Fig. (4). As a time-dependent material, the higher the aging time, the larger is the static yield stress, as observed in the comparison to the blue color curves of Fig. (5). However, the higher the aging time, the smaller the rate of increase in the yield stress. Furthermore, once the static yield stress reached 550 Pa, the black-squared curve reveals that the material structure is substantially stronger in comparison to dynamically formed hydrate slurries. Even though yield stress increases with aging time, yield stress measured after a dynamic hydrate formation cannot reach the counterpart obtained after a static formation.

4. CONCLUSIONS

The main conclusions can be summarized as follows:

- The higher the imposed shear rate during cooling period, the shorter is the induction time and the faster the material reached the steady state;
- The apparent viscosity of hydrate slurry is at least 1 order of magnitude larger than the brine fluid apparent viscosity;
- The THF-hydrate slurry in brine fluid can be described as an elasto-viscoplastic, irreversible time-dependent material as the material yield stress and, elasticity at low deformations degrades irreversibly with shear;

These findings may bring new perspectives for the flow startup, especially, the material brittleness, the shear influence on the hydrate formation, and the shear degradation of the microstructure.

5. ACKNOWLEDGEMENTS

The authors acknowledge the financial support of PETROBRAS S/A (TC 0050.0070318.11.9), CNPq (process: 487091/2013-2), CAPES, FINEP, PRH, and PFRH/PETROBRAS (6000.0067933.11.4 and 6000.0082166.13.4). The authors also thank the Multilab LabReo-CERNN/UTFPR for providing the rheometers used in the current work.

6. REFERENCES

Ahuja, A., Zylyftari, G., & Morris, J. F., 2015. “Yield stress measurements of cyclopentane hydrate slurry.” *Journal of Non-Newtonian Fluid Mechanics*, Vol. 220, pp. 116-125.

Bavoh, C. B., Ofei, T. N., & Lal, B., 2020. “Investigating the potential cuttings transport behavior of ionic liquids in drilling mud in the presence of sII hydrates”. *Energy & Fuels*, Vol. 34, No. 3, pp. 2903-2915.

Botrel, T., 2001. “Hydrates prevention and removal in ultra-deepwater drilling systems.” In *Offshore Technology Conference*. OnePetro.

de Lima Silva, P. H., Naccache, M. F., de Souza Mendes, P. R., Campos, F. B., Teixeira, A., & Sum, A. K., 2017. “Rheology of tetrahydrofuran hydrate slurries.” *Energy & Fuels*, Vol. 31, No. 12, pp. 14385-14392.

Hammerschmidt, E. G., 1934. “Formation of gas hydrates in natural gas transmission lines.” *Industrial & Engineering Chemistry*, Vol. 26, No.8, pp. 851-855.

Iida, Tomoyuki, Mori, H., Mochizuki, T., and Mori, Y. H., 2001. “Formation and dissociation of clathrate hydrate in stoichiometric tetrahydrofuran–water mixture subjected to one-dimensional cooling or heating.” *Chemical engineering science*, Vol. 56, No. 16, pp. 4747-4758.

Kelland, M. A., Mønig, K., Iversen, J. E., & Lekvam, K., 2008. “Feasibility study for the use of kinetic hydrate inhibitors in deep-water drilling fluids.” *Energy & Fuels*, Vol. 22, No. 4, pp. 2405-2410.

Liu, W., Hu, J., Sun, Z., Chu, H., Li, X., & Sun, F., 2019. “Research on evaluation and prevention of hydrate formation and blockage risk in wellbore during deepwater gas wells drilling.” *Journal of Petroleum Science and engineering*, Vol. 180, pp.668-680.

Østergaard, K. K., Tohidi, B., Danesh, A., & Todd, A. C., 2000. “Gas hydrates and offshore drilling: predicting the hydrate free zone.” *Annals of the New York Academy of Sciences*, Vol. 912, No. 1, pp. 411-419.

Peixinho, J., Karanjkar, P. U., Lee, J. W., & Morris, J. F., 2010. “Rheology of hydrate forming emulsions.” *Langmuir*, Vol. 26, No. 14, pp. 11699-11704.

Qin, Y., Aman, Z. M., Pickering, P. F., Johns, M. L., & May, E. F., 2017. “High pressure rheological measurements of gas hydrate-in-oil slurries”. *Journal of Non-Newtonian Fluid Mechanics*, Vol. 248, pp. 40-49.

Sloan, E. D., 2005. “A changing hydrate paradigm—from apprehension to avoidance to risk management.” *Fluid Phase Equilibria*, Vol. 228, pp. 67-74.

Sloan Jr, E. D., & Koh, C. A., 2007. *Clathrate hydrates of natural gases*. CRC press, 3rd edition.

Sloan, E. D. (2010). *Natural gas hydrates in flow assurance*. Gulf Professional Publishing.

7. RESPONSIBILITY NOTICE

The author(s) is (are) the only responsible for the printed material included in this paper.